

# 14A2 Estimating Vortex Center Locations and Movements in Four-Dimensional Space From Radar Observed Tornadoic Mesocyclones

Qin Xu<sup>1\*</sup>, Li Wei<sup>2</sup> and Kang Nai<sup>2</sup>

<sup>1</sup>NOAA/National Severe Storms Laboratory, Norman, Oklahoma

<sup>2</sup>Cooperative Institute for Mesoscale Meteorological Studies, University of Oklahoma

## 1. Introduction

Gao et al. (2013) adapted a real-time three-dimensional variational data assimilation (3DVar) system to diagnose storm wind fields from multiple Doppler radar observations. This 3DVar system can identify storm-scale mid-level circulations, but the circulation may not be fully resolved due to the isotropic univariant background covariance used for each velocity component in the cost-function. To improve the mesocyclone wind analyses, a new variational method is developed by formulating the background covariance with desired vortex-flow dependences in a moving frame following the mesocyclone on each selected tilt of radar scan (Xu et al. 2015). The method can be extended to analyze three-dimensional vortex winds from either single-Doppler or multi-Doppler scans of mesocyclones with the background wind error correction functions formulated in a slantwise cylindrical coordinate system co-centered with the mesocyclone at each vertical level. For this extension, the first task is to estimate the vortex center location of the detected mesocyclone as a continuous function of height and time in the four-dimensional space. To accomplish this task, a multi-step method is developed. The method is applied to the tornadoic mesocyclone observed by operational radars in Oklahoma on 20 May 2013. The detailed steps of the method and their performances with the above tornadoic mesocyclone case are reported in this paper.

## 2. Multi-step method

The method consists of the following three steps: First, the mesocyclone area is identified as a by-product of the mesocyclone-targeted radar velocity dealiasing and the mesocyclone vortex center location is also estimated as a by-product to provide an initial guess of the vortex center location on each tilt of radar scan. Then, a two-step algorithm is applied to the dealiased radial-velocity field in the mesocyclone area to further estimate the vortex center location on each tilt. Finally, the mesocyclone vortex center location is estimated as a continuous function of height and time by fitting a smooth-function form constructed by B-spline basis functions to the vortex center locations estimated in the second step. The estimated function is denoted by  $\mathbf{x}_c(z, t)$  where  $\mathbf{x}_c \equiv (x_c, y_c)$ . The detailed techniques used in the above steps are described in the following sections.

## 3. Mesocyclone-targeted velocity dealiasing in step-1

In this first step, the mesocyclone area is identified as a by-product of the mesocyclone-targeted velocity dealiasing with the vortex center location estimated as the first guess on each

tilt. The mesocyclone-targeted velocity dealiasing contains an additional step beyond those reported in Xu et al. (2013). In this additional step, the alias-robust least-squares method with a two-parameter vortex model for correcting aliased radial-velocity data around a hurricane (Xu et al. 2014) is extended into an alias-robust variational method with a 6-parameter vortex model for correcting aliased radial-velocity data around a mesocyclone.

In the above extension, the radial velocity is expressed by

$$\begin{aligned} v_{ri} &= v_r(r_i, \phi_i, \theta_i | V_M, R_M, r_c, \phi_c, V_e, \beta) \\ &\equiv V_e \cos(\phi_i - \beta) + V_T \sin(\alpha_i - \phi_i) \cos \theta_i. \end{aligned} \quad (1)$$

Here,  $r_i$ ,  $\phi_i$  and  $\theta_i$  denote the radial distance, azimuthal and elevation angles of the  $i^{\text{th}}$  observation point, respectively, in the radar coordinates.  $V_M$  is the maximum tangential velocity of the modeled vortex, and  $R_M$  is the radius of  $V_M$  from the vortex center.  $r_c$  and  $\phi_c$  denote the radial distance and azimuthal angle of the vortex center, respectively, in the radar coordinates.  $V_e$  and  $\beta$  denote the environmental wind speed and direction angle (with respect to the northward  $y$ -coordinate). The radial profile of vortex tangential velocity is described by the following parametric vortex model (Vatistas et al. 1991):

$$V_T(R) = V_M(R/R_M)[1/2 + (R/R_M)^4/2]^{1/2},$$

where  $R$  is the radius distance to the vortex center. Thus,  $V_{Ti} = V_T(R_i)$  is the modeled vortex tangential velocity at  $R = R_i$ , where  $R_i$  is the radius distance of the  $i^{\text{th}}$  observation point from the vortex center and is computed as a function of  $(r_i, \phi_i, r_c, \phi_c)$  by (4b) of Xu et al. (2014).  $\alpha_i$  is the azimuthal angle of the  $i^{\text{th}}$  observation point viewed from the vortex center and is computed as a function of  $(r_i, \phi_i, r_c, \phi_c)$  by (4c) of Xu et al. (2014).

The expression of  $v_{ri}$  in (1) is used to fit aliased radial velocity observations  $v_{ri}^o(r_i, \phi_i, \theta_i)$  directly. The fitting minimizes the following cost-function:

$$J = \sum_i \{Z[v_{ri} - v_{ri}^o, v_N]\}^2, \quad (2)$$

where  $\sum_i$  denotes the summation over  $i$ ,  $Z[(\cdot), v_N] \equiv (\cdot) - 2v_N \mathcal{N}[(\cdot), v_N]$  is the aliasing operator,  $v_N$  is the Nyquist velocity,  $\mathcal{N}[(\cdot), v_N] \equiv \text{Int}[(\cdot)/(2v_N)]$  is the Nyquist number of  $(\cdot)$ ,  $\text{Int}[(\cdot)]$  represents the nearest integer of  $(\cdot)$ . The cost-function in (1) is formulated based on the unconventional approach (Xu et al. 2009, Xu 2009) and thus is smooth and concave upwards in the vicinity of the global minimum. The global minimum is difficult to found by the conjugate-gradient descent algorithm in the space of  $(V_M, R_M, r_c, \phi_c, V_e, \beta)$  unless the initial guess is sufficiently close to the global minimum. To overcome this difficulty, a brut-force search is

\* Corresponding author address: Qin Xu, National Severe Storms Laboratory, 120 David L. Boren Blvd., Norman, OK 73072-7326; E-mail: Qin.Xu@noaa.gov

used in the subspace of  $(V_M, R_M)$  by selecting  $5 \times 5$  guesses of  $(V_M, R_M)$  around the initial guess of  $(V_M, R_M)$ . The conjugate-gradient descent algorithm is then used to search the conditional global minimum in the subspace of  $(r_c, \phi_c, V_e, \beta)$  with  $(V_M, R_M)$  fixed to each of the  $5 \times 5$  guesses. The smallest of the  $5 \times 5$  conditional minima in  $(r_c, \phi_c, V_e, \beta)$  gives a close estimate of the global minimum in  $(V_M, R_M, r_c, \phi_c, V_e, \beta)$ .

The above additional step of dealiasing (beyond those reported in, the mesocyclone-targeted velocity dealiasing is more effective than the previous technique (Xu et al. 2013) in detecting and correcting the aliased radial-velocity data within each mesocyclone. The improvement is exemplified by the comparison in Fig. 1.

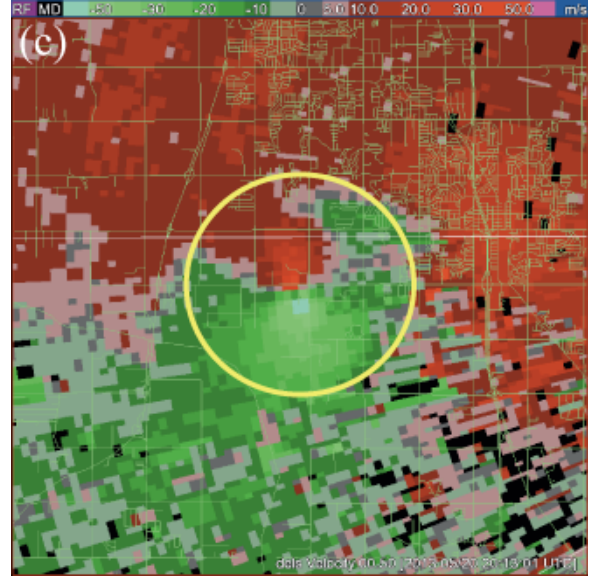
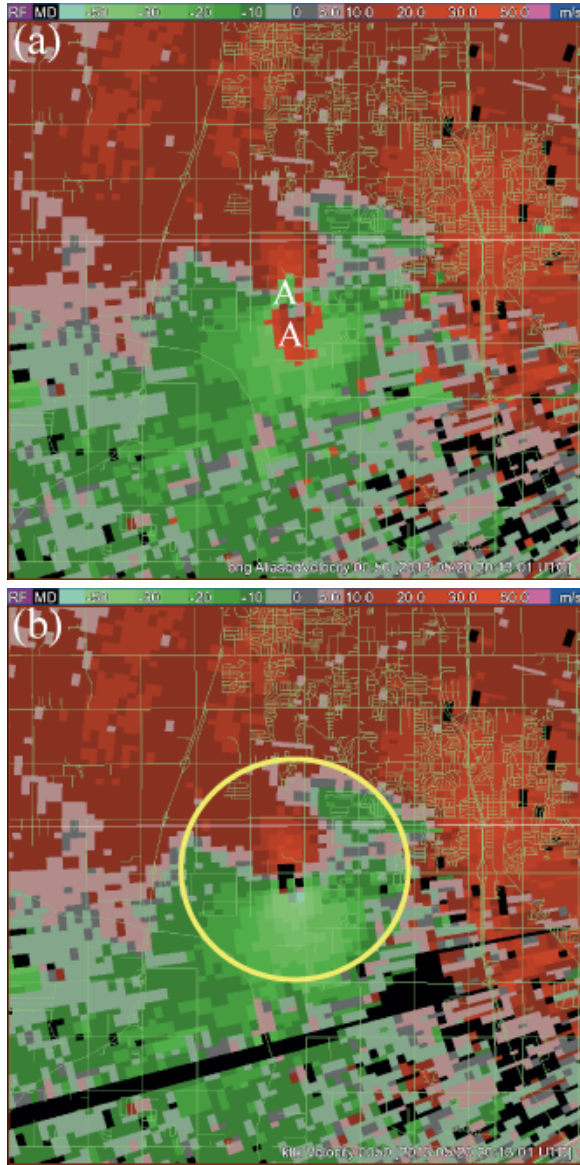


Fig. 1. (a) Image of raw radial velocity (superimposed on the Moore city street map plotted by bright green lines) scanned from KTLX radar on  $0.5^\circ$  tilt at 20:13:01 UTC on 20 May 2013 for the Moore, Oklahoma tornadic storm. (b) Image of dealiased radial velocity produced by the previous method (Xu et al. 2013). (c) Image of dealiased radial velocity produced by the mesocyclone-targeted velocity dealiasing with the above explained additional step to detect and correct severely aliased radial-velocity data around each tornadic mesocyclone. The white letters “A” in (a) mark the aliased-velocity areas. The yellow circle in (b) and (c) encircles the mesocyclone and its produced EF5 tornado. The black pixels within the yellow circle in (b) show the flagged (missed) data in the vortex center area.

#### 4. Estimating vortex center location on each tilt in step-2

The vortex center location  $(r_c, \phi_c)$  estimated in the radar coordinates as a by-product of the mesocyclone-targeted velocity dealiasing in the previous section is used here as the first guess. From this first guess, the vortex center location is re-estimated by applying the following two-step algorithm to the dealiased radial-velocity field in the mesocyclone area on each tilt:

- I. The initial estimate of vortex center is the point  $(r_c^0, \phi_c^0)$  at which the azimuthal shear of  $v_r^0$  is largest within the sector of 20 km arc length and 20 km radial range centered at the first guess point in the mesocyclone area.
- II. The final estimate of the vortex center location is given by

$$(r_c, \phi_c) = \sum_j (r_j, \phi_j) w_j / \sum_j w_j,$$

where  $w_j = (\Delta v_{rj} / \Delta l_j)^2$  is the weight,  $(\Delta l_j)^2 = (r_j - r_c^0)^2 + r_j^2 (\phi_j - \phi_c^0)^2$ , and  $\sum_j$  denotes the summation over  $j$  for up to five range circles that have the first five largest values of  $\Delta v_{rj}$ .

The above two-step algorithm is applied to 10 consecutive volumes of radial-velocity data scanned by operational KTLX from 1951 to 2035 UTC for the Oklahoma Moore tornadic mesocyclone on 20 May 2013. The estimated values of  $(r_c, \phi_c)$  in the radar coordinates are converted to the values of  $(x_c, y_c)$  in the Cartesian coordinates with the origin  $(x, y) = (0, 0)$

at the vortex center estimated on the first (lowest) tilt in the first volume of the aforementioned 10 consecutive volume scans. These 10 consecutive volume scans is covered by the time period of  $0 \leq t \leq T = 55$  min while  $t = 0$  corresponds to 1941 UTC, that is, 10 minutes before the starting time (1951 UTC) of the first volume scan. The estimated values of  $x_c$  (or  $y_c$ ) are shown by the numbers (in km) at discrete points of  $(z, t)$  in Fig. 2a (or Fig. 2b), where each discrete point of  $(z, t)$  corresponds to the height and time at which the vortex center is estimated (on each tilt in each volume).

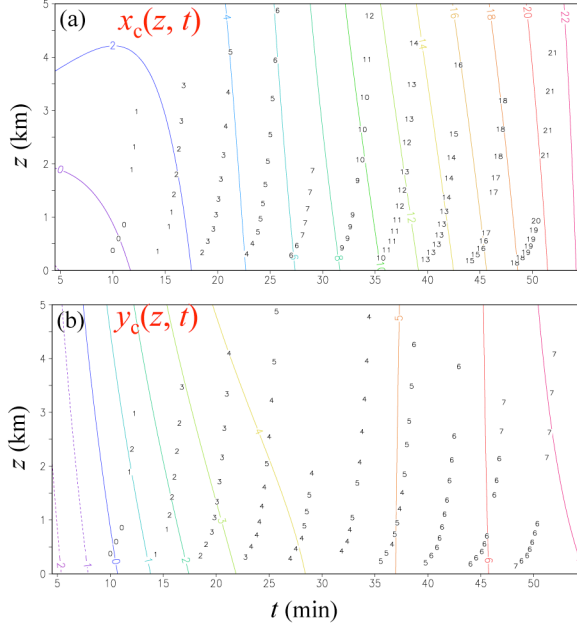


Fig. 2. (a) Values of  $x_c$  estimated by the two-step algorithm shown by the numbers (in km) at discrete points of  $(z, t)$ , and the continuous function  $x_c(z, t)$  estimated by the fitting in section 5 shown by the colored counters. (b) As in (a) but for values of  $y_c$  at discrete points of  $(z, t)$  and the continuous function  $y_c(z, t)$  estimated by the fitting in section 5.

### 5. Estimating $\mathbf{x}_c(z, t)$ in step-3

The vortex center location  $\mathbf{x}_c = (x_c, y_c)$  is estimated as a continuous function of  $(z, t)$  by fitting  $\mathbf{x}_c(z, t)$  constructed by B-spline basis functions to the vortex center locations estimated in the previous section. In particular, the fitting minimizes the following cost functions:

$$J(a_{kn\beta}) = \sum_i [x_c(z_i, t_i | a_{kn\beta}) - x_{ci}]^2,$$

$$J(b_{kn\beta}) = \sum_i [y_c(z_i, t_i | b_{kn\beta}) - y_{ci}]^2,$$

where  $\sum_j$  denotes the summation over  $i$ ,  $x_c(z_i, t_i | a_{kn\beta}) = \sum_{kn\beta} a_{kn\beta} B_k(z_i) B_n^\beta(t_i)$ ,  $y_c(z_i, t_i | b_{kn\beta}) = \sum_{kn\beta} b_{kn\beta} B_k(z_i) B_n^\beta(t_i)$ ,  $\sum_{kn\beta}$  denotes the summation over  $k, n$  and  $\beta$ ,  $B_k(z)$  denotes the linear basis function at the  $k^{\text{th}}$  node point in  $z$ ,  $B_n^\beta(t)$  denotes the quadratic basis function of  $\beta^{\text{th}}$  order (with  $\beta = 0, 1$ ) at the  $n^{\text{th}}$  node point in  $t$ , and  $\mathbf{x}_{ci} = (x_{ci}, y_{ci})$  denotes the  $i^{\text{th}}$  vortex center location estimated at  $(z_i, t_i)$  by the two-step algorithm in the previous section. The quadratic basis function  $B_n^\beta(t)$  with the  $n^{\text{th}}$  node point at  $t = 0$  is shown by the red (or green) curve for  $\beta = 0$  (or  $\beta = 1$ ) in Fig. 3.

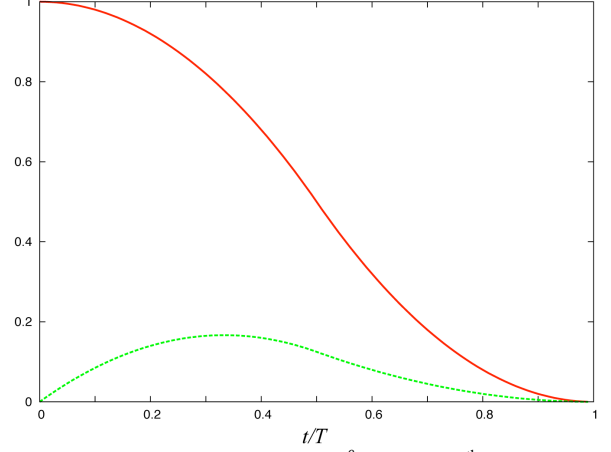


Fig. 3. Quadratic basis function  $B_n^\beta(t)$  for the  $n^{\text{th}}$  node point at  $t = 0$  plotted by the red (or green) curve for  $\beta = 0$  (or  $\beta = 1$ ). The time  $t$  is scaled by  $T = 55$  min.

The above fitting is applied to all the  $\mathbf{x}_{ci} = (x_{ci}, y_{ci})$  estimated in the previous section for the 10 consecutive volumes of radial-velocity data scanned by operational KTLX for the Oklahoma Moore tornadic mesocyclone on 20 May 2013. The vertical domain of  $0 \leq z \leq 5$  km is covered by a single element with the linear basis function, and the time domain of  $0 \leq t \leq 55$  min is covered by a single element with the quadratic basis function. The estimated continuous function  $x_c(z, t)$  [or  $y_c(z, t)$ ] is shown by the colored counters in Fig. 2a (or Fig. 2b). The trajectory of the estimated  $\mathbf{x}_c(0, t)$  at the surface level ( $z = 0$ ) is plotted by the dashed green curve in Fig. 4, where the nine colored line segments show how the estimated  $\mathbf{x}_c(z, t)$  varies with  $z$  (from 0 to 5 km) at nine different times. As shown, the estimated vortex center location is slanted away from the vertical  $z$ -direction at each fixed time, and the slanted vortex core became more vertical as the vortex intensified and moved toward and into city Moore in the later time (around  $t = 45$  min or 2025 UTC).

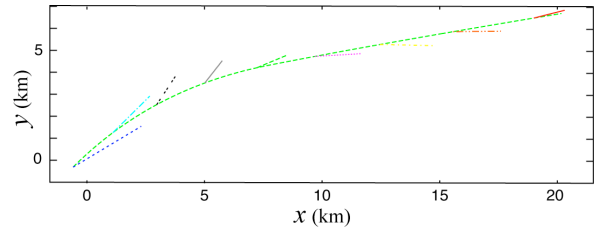


Fig. 4. Trajectory of the estimated  $\mathbf{x}_c(0, t) = [x_c(0, t), y_c(0, t)]$  at the surface level ( $z = 0$ ) plotted by the dashed green curve. The colored line segments started from nine different points (for nine different times) along the green trajectory show how the estimated  $\mathbf{x}_c(z, t)$  vary with  $z$  (from 0 to 5 km) at the nine different times.

Using the estimated  $\mathbf{x}_c(z, t)$ , the background error covariance functions can be formulated with desired vortex-flow-dependences in the three-dimensional space for any given time (within the time window of  $0 \leq t \leq 55$  min), so the two-dimensional vortex wind analysis of Xu et al. (2015) can be extended to a three-dimensional vortex wind analysis in a slantwise cylindrical coordinate system co-centered with the

the estimated  $\mathbf{x}_c(z, t)$  at a given  $t$ . As an example, the analyzed axi-symmetric part of the three-dimensional vortex in the slantwise cylindrical coordinates ( $z'$ ,  $r$ ) at  $t = 15$  min (or 45 min) is shown in Fig. 5a (or 5b).

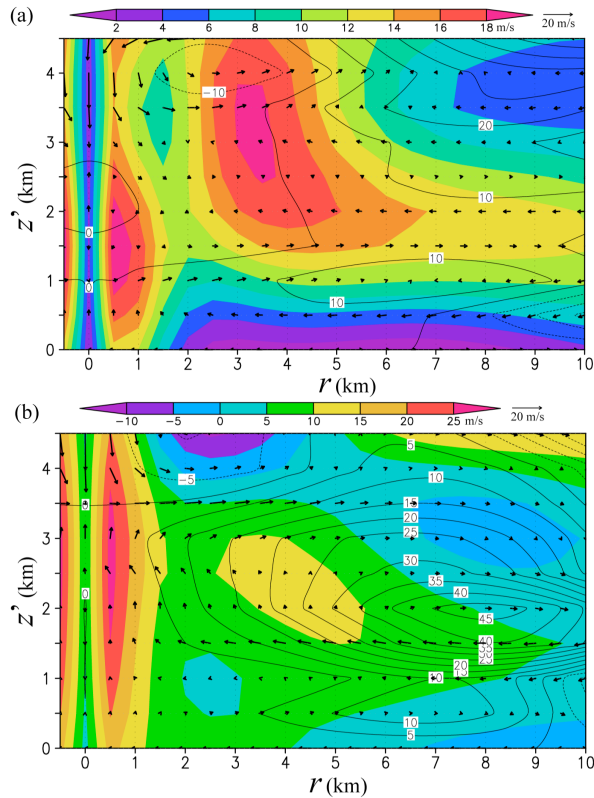


Fig. 5. (a) Vertical cross-section for the axi-symmetric part of the three-dimensional vortex in the slantwise cylindrical coordinates ( $z'$ ,  $r$ ) at  $t = 15$  min, where the color scale is for the tangential velocity, and the black arrows (or contours) plot the velocity (or stream function) of the vertical circulation. (b) as in (a) but for the vertical cross-section at  $t = 45$  min.

## 6. Conclusions

A multi-step method is developed to estimate the vortex center location of radar observed mesocyclone in the four-dimensional space. The estimated vortex center location is a continuous function of height and time, denoted by  $\mathbf{x}_c(z, t)$  where  $\mathbf{x}_c \equiv (x_c, y_c)$ . This estimated function  $\mathbf{x}_c(z, t)$  provides the first necessary and critical information for extending the two-dimensional vortex wind analysis of Xu et al. (2015) to a three-dimensional vortex wind analysis in a slantwise cylindrical coordinate system co-centered with the estimated  $\mathbf{x}_c(z, t)$  at a given  $t$ . The multi-step method is successfully applied to the tornadic mesocyclone observed by operational radars in Oklahoma on 20 May 2013.

The estimated  $\mathbf{x}_c(0, t)$  at the surface level ( $z = 0$ ) can be used in an additional step to timing the tornado damage survey data, so the possible cycloid movement of vortex center can be detected and estimated at the surface level from the tornado damage survey data. The research progress and preliminary results obtained in this direction can be found from the recorded oral presentation of 14A2 posted at the AMS conference web site. The cycloid pattern revealed by the

tornado damage survey data seems to suggest that the tornado vortex could be a satellite vortex moving circularly within the mesocyclone and around the center of the mesocyclone. The cycloid pattern revealed by the tornado damage survey data could be also partially caused by rear-flank downdraft surges according to Kurdzo et al. (2015). Clarifying these possible features and resolving the detailed three-dimensional vortex flows require continued research and development in vortex wind analyses with rapid-scan radar observations.

## Acknowledgments

The research work was supported by the ONR Grant N000141410281 to the University of Oklahoma (OU). Funding was also provided to CIMMS by NOAA/Office of Oceanic and Atmospheric Research under NOAA-OU Cooperative Agreement #NA17RJ1227, U.S. Department of Commerce.

## REFERENCES

- Burgess, D., K. Ortega, G. Stumpf, G. Garfield, C. Karstens, T. Meyer, B. Smith, D. Spehger, J. Ladue, R. Smith, and T. Marshall, 2014: 20 May 2013 Moore, Oklahoma, tornado: Damage survey and analysis. *Wea. Forecasting*, **29**, 1229–1237.
- Gao, J., T. M. Smith, D. J. Stensrud, C. Fu, K. Calhoun, K. L. Mnaross, J. Brogden, V. Lakshmanan, Y. Wang, K. W. Thomas, K. Brewster, and M. Xue, 2013: A realtime weather-adaptive 3DVAR analysis system for severe weather detections and warnings. *Wea. Forecasting*, **28**, 727–745.
- Kurdzo, J. M., D. J. Bodine, B. L. Cheong, and R. D. Palmer, 2015: High-temporal resolution polarimetric X-band Doppler radar observations of the 20 May 2013 Moore, Oklahoma, tornado. *Mon. Wea. Rev.*, **143**, 2711–2735.
- Xu, Q., 2009: Bayesian perspective of the unconventional approach for assimilating aliased radar radial velocities. *Tellus*, **61A**, 631–634.
- Xu, Q., Y. Jiang, and L. Liu, 2014: Fitting parametric vortex to aliased Doppler velocities scanned from hurricane. *Mon. Wea. Rev.*, **142**, 94–106.
- Xu, Q., K. Nai, S. Liu, C. Karstens, T. Smith and Q. Zhao, 2013: Improved Doppler velocity dealiasing for radar data assimilation and storm-scale vortex detection. *Advances in Meteorology*, vol. **2013**, Article ID 562386, 10 pages.
- Xu, Q., L. Wei, and S. Healy, 2009: Measuring information content from observations for data assimilations: connection between different measures and application to radar scan design. *Tellus*, **61A**, 144–153.
- Xu, Q., L. Wei and K. Nai, 2015: Analyzing vortex winds in radar observed tornadic mesocyclones for nowcast applications. *Wea. and Forecasting*, **30**, 1140–1157.